Genomics of Neotropical biodiversity indicators: two butterfly radiations with rampant chromosomal rearrangements and hybridisation

Eva SM van der Heijden[1,2], Karin Näsvall[1], Carlos Eduardo Beserra Nobre[3], Fernando A. Seixas[4], Artur Campos D Maia[3,5], Patricio Salazar-Carrión[1,2], Jonah M Walker[1,2], Daiane Szczerbowski[6], Stefan Schulz[6], Ian A Warren[2], Kimberly Gabriela Gavilanes Córdova[7], María José Sánchez-Carvajal[7], Franz Chandi[7], Alex P Arias-Cruz[7], Nicol Rueda-M[1,8], Camilo Salazar[8], Kanchon K Dasmahapatra[9], Stephen H Montgomery[10], Melanie McClure[11], Dominic E Absolon[1], Thomas C Mathers,[1] Camilla A Santos[1], Shane McCarthy[1], Jonathan MD Wood[1], Caroline Bacquet[8,12], André Victor Lucci Freitas[13], Keith R. Willmott[14], Chris D Jiggins[2], Marianne Elias[12,15], Joana I Meier[1,2]

1. Tree of Life Programme, Wellcome Sanger Institute, UK
2. Department of Zoology, University of Cambridge, UK
3. Graduate Program in Animal Biology, Federal University of Pernambuco, Brazil
4. Department of Organismic and Evolutionary Biology, Harvard University, Cambridge, MA, USA
5. Graduate Program in Plant Biology, Federal University of Pernambuco, Brazil
6. Institute of Organic Chemistry, Technische Universität Braunschweig, Germany
7. Universidad Regional Amazónica Ikiam, Ecuador
8. Biology Program, Faculty of Natural Sciences, Universidad del Rosario, Bogotá, Colombia
9. Department of Biology, University of York, UK
10. University of Bristol, UK
11. Laboratoire Écologie, Évolution, Interactions des Systèmes Amazoniens (LEEISA), Université de Guyane, CNRS, IFREMER, Cayenne, France
12. Smithsonian Tropical Research Institute, Gamboa, Panama
13. Universidade Estadual de Campinas, Brazil
14. Florida Museum of Natural History, USA
15. Institut de Systématique Évolution Biodiversité (ISYEB), CNRS, MNHN, EPHE, Sorbonne Université, Université des Antilles, Paris, France

Author contributions:

PSC, JIM, ESMH, KGGC, MJSC, DS, FC, APAC, CB, NRM, CS, KKD, NN, SHM, MM, KRW, AVLF, CDJ and ME collected samples. KRW and ME oversaw the butterfly identification. ESMH, JIM, JMW and IAW performed lab work. ESMH mapped and filtered the sequencing data, and ran the phylogenetic and hybridisation analyses. KN did the chromosomal rearrangement analysis. CEBN, ACDM, DS, SS and AVLF analysed the androconial semiochemicals. FAS ran the MSCi analysis. DEA, TCM, CAS, SM, KN and JW assembled and curated the new genomes. JIM designed the study with contributions from ESMH, ME and CDJ. ESMH, JIM and KN wrote the manuscript with contributions from all authors.

Corresponding author: Joana Isabel Meier, joana.meier@sanger.ac.uk

Key words:

Speciation, biodiversity, butterflies, neotropics, genomics

Classification:

Biological Sciences - Evolution

Abstract

A major question in evolutionary biology is what drives the diversification of lineages. Rapid, recent radiations are ideal systems for addressing how new species arise because they may preserve key morphological and ecological adaptations associated with speciation. *Melinaea* and *Mechanitis* are two classic examples of rapidly radiating Neotropical butterfly genera of the tribe Ithomiini. They were models for early studies of Amazonian biogeography and colour pattern mimicry and have been proposed as biodiversity indicators. We generated reference genomes for five species of each genus, and whole-genome resequencing data of most species and subspecies covering a wide geographic range to assess phylogeographic relationships, patterns of hybridisation and chromosomal rearrangements. We find rampant evidence of hybridisation within both radiations, which may have facilitated their rapid diversification. Our data also provide evidence for a putative hybrid species that combines traits of both parental species. Moreover, many chromosomal fusions and fissions were identified, even between sister species. Our data also help resolve the classification of these notoriously taxonomically challenging butterflies. We conclude that interactions between geography, hybridisation and chromosomal rearrangements have contributed to these two rapid radiations in the highly diverse Neotropical region.

Introduction

Rapid adaptive radiations, where a lineage diversifies into many ecologically different species over a short time period, are ideal systems for studying rapid adaptation and how new species evolve (1, 2). Coexistence between the adaptive radiation lineages requires adaptation to different ecological niches and some reproductive isolation that prevents the incipient species from merging. While the availability of niches is thus a key requirement, there are lineage-specific factors that determine which lineage will use these niches and undergo adaptive radiation (3). Factors that increase the speed of adaptation or reproductive isolation are thus good candidates for drivers of adaptive radiation.

For instance, while gene flow between divergent lineages can homogenise their gene pools, recent studies have shown that sometimes hybridisation can facilitate rapid diversification by introducing adaptive genetic variants or incompatibilities to one or both parental lineages (4, 5). Admixture has been shown to kickstart adaptive radiation (e.g. 6, 7), facilitate parallel adaptation (e.g. 5, 8), novel adaptations (e.g. 9) or hybrid speciation (10).

High rates of karyotype changes can speed up the accumulation of reproductive isolation barriers (11–14), and many lineages with rapid radiations also display high chromosomal instability (15–17). However, the extent to which chromosomal rearrangements contribute to speciation remains an open

question. Offspring from parents with different karyotypes may suffer reduced fitness (18), due to mismatch in pairing of homologous chromosomes that results in aneuploidy, meiotic failure or hybrid sterility (19). Chromosomal rearrangements can also facilitate divergence in the face of gene flow if they link together co-adapted variants (20, 21).

Periods of geographic separation, e.g. due to climatic oscillations fragmenting suitable habitat, followed by secondary contact have been proposed to facilitate species radiations as they allow the accumulation of differences in the absence of gene flow and upon secondary contact, speciation may progress through reinforcement of reproductive isolation, ecological character displacement or admixture leading to novelty (22). For instance, in the Neotropics, both the formation of the Andes and forest refugia in the Quaternary have been proposed as "speciation pumps" (23) .

Here, we study whether these factors contribute to rapid diversification in two Neotropical butterfly radiations of the tribe Ithomiini (Nymphalidae: Danainae). Ithomiine butterflies are found across Central and South America, from sea level up to cloud forests at 3000 metres (24). The tribe consists of 42 genera with over 390 species, peaking in species richness in Western Amazonia and the eastern slopes of the Andes (24, 25). Ithomiine butterflies are regarded as potential indicators of spatial patterns in biodiversity in the Neotropics, one of the most biodiverse areas in the world (24, 26, 27). Sequestration of pyrrolizidine alkaloids (PA) from Asteraceae and Boraginaceae plants render most Ithomiini unpalatable (28–32), and their conspicuous colour patterns advertise this unpalatability to predators. They form Müllerian mimicry rings, where different taxa share the cost of educating predators by resembling each other (33, 34).

We focus on two ithomiine genera, *Melinaea* and *Mechanitis*, that have diversified exceptionally fast with most species younger than a million years (25, 35). They are thought to form adaptive radiations as the species show differences in microhabitats, host plants, mimicry rings, and altitude (36–40). While it is unknown why they radiated so fast, different contributing factors have been proposed. Allopatric speciation may have occurred in different rainforest refugia in the Quaternary (41, 42, but see 43) or after crossing the Andes. There is some evidence for hybridisation (e.g. 44) but its role in speciation is unknown. Chromosomal differences may also have contributed to speciation as chromosome counts range from 13 to 30 chromosomes (45). Chromosomal rearrangements likely contribute to reproductive isolation, as has been shown in a cross between two *Melinaea* species with nearly sterile hybrids (46). However, intraspecific variation in chromosome counts (45, 46) indicates that not all rearrangements reduce fitness strongly. Some species also differ in male-specific androconial compounds, which may act as pheromones

contributing to assortative mating (47, 48), facilitating reinforcement of species boundaries upon secondary contact (49).

The study of these radiations has been hampered by taxonomic challenges. The species do not differ in genital or other morphological characteristics and show substantial intraspecific wing pattern variation and mimicry between taxa. They are thus among the most taxonomically challenging of Ithomiini; as Fox has stated (1967): 'these insects [are] so thoroughly confusing and so thoroughly confused by my predecessors'. Barcoding does not reliably distinguish species either (44, 50). They have thus undergone many taxonomic revisions (e.g. 37, 42, 45, 46, 50–54).

Here, we use five reference genomes of each genus and whole-genome resequencing data of almost all species and many subspecies, to resolve taxonomic uncertainties and explore whether admixture or chromosomal rearrangements may have played a role in the rapid diversification of *Mechanitis* and *Melinaea* butterflies.

Results

Taxonomic revision

Through whole-genome resequencing of 135 *Mechanitis* and 107 *Melinaea* individuals from across South and Central America, with additional individuals from the outgroup genera *Forbestra*, *Eutresis* and *Olyras*, we shed light on the phylogenomic relationship of the subspecies and species status (**Fig. 1**). Our results confirm species versus subspecies status for most known taxa according to (54), support two recent species reclassifications (*Mel. tarapotensis* (46), *Mel. mothone* (55)) and reveal three additional taxa that need to be elevated to species level (*Mel. maeonis* **stat rest** (Hewitson 1869), *Mec. nesaea* **stat rest** (Hübner 1820), *Mec. macrinus* **stat rest** (Hewitson 1860), **Fig. 1**; **Text S1**).

Mitonuclear discordance

In both *Mechanitis* and *Melinaea*, we find rampant mitonuclear discordance, *i.e.* mismatches between mitochondrial and nuclear phylogenies (**Fig. 1**). For instance, *Mec. nesaea* is sister to *Mec. polymnia* in the nuclear phylogeny, but to *Mec. lysimnia* in the mitochondrial phylogeny (**Fig. 1A - box III; Fig. S1-2**). This result could be indicative of admixture (more details below). *Mec. messenoides* harbours two divergent mitochondrial haplotypes, as found previously (37, 44) (**Fig. 1A - box II**), one clustering with the *polymnia-lysimnia* clade, and the other one with its sister species in the nuclear phylogeny, *Mec. menapis*. The mitochondrially divergent *Mec. messenoides* individuals do not form separate clades in the nuclear

phylogeny, nor do they differ in collection location or subspecies (**Table S1; Fig. S1-2**). They may thus indicate ancient admixture.

While the *Melinaea* species are clearly differentiated in the nuclear phylogeny, the mitochondrial phylogeny shows almost no variation among species, confirming previous barcoding results (55) (**Fig. 1B; Fig. S3-4**). Apart from *Mel. ludovica*, *Mel. tarapotensis* and *Mel. lilis*, all species form part of the same shallow mitochondrial clade with no species differentiation. Interestingly, *Mel. ludovica* is the only one that is also an outgroup to the rest of the *Melinaea* species in the nuclear phylogeny, whereas *Mel. lilis* and *Mel. tarapotensis* are sister to *Mel. isocomma* and *Mel. satevis* in the nuclear phylogeny, respectively.

Phylogeographic patterns

By combining our sampling locations with those compiled by (24) adjusted according to our taxonomic revision (**Fig. 2**), we assessed the potential role of allopatry in speciation. We find four main biogeographic regions (**Fig. 2**), with most species restricted to one of them. The Andes separate some of the *Mechanitis* sister species (**Fig. 2A**). *Mec. messenoides* and *Mec. mazaeus* are found east of the Andes (Western Amazonia) and their respective sister species *Mec. menapis* and *Mec. macrinus* are found west of the Andes. Within *Mec. polymnia*, Ecuadorian and Colombian individuals from opposite sides of the Andes are highly divergent, indicating little gene flow. This pattern of species separation by the Andes was not previously as apparent due to species misclassification.

In *Melinaea*, only two species included in our dataset occur west of the Andes (*Mel. lilis* and *Mel. idae*) and they form a clade with a third species occurring east of the Andes (*Mel. isocomma*). Our dataset lacks a potential third species occurring west of the Andes, *Mel. scylax* (24), which may represent a subspecies of *Mel. lilis* (42, 56). Other potential species missing in our dataset are *Mel. mnemopsis* from Western Amazonia, *Mel. ethra* from the Atlantic forest and *Mel. mnasias* from Western Amazonia and the Atlantic Forest (24, 56), and we are missing some subspecies that might turn out to be better classified as another species (e.g. *Mel. menophilus mediatrix* from French Guiana (55)). Most of the individuals in our *Melinaea* dataset are from Western Amazonia (east of the Andes) and we find that many sister species are sympatric.

Calibrated phylogenetic tree

A time-calibrated phylogeny using divergence times from (25) as secondary calibration points (**Fig. 2A; Fig. S7A**) showed that the seven *Mechanitis* species have diversified within the past 1.67 million years, resulting in a speciation rate of at least 1.165 speciation events per lineage/My (assuming a pure birth

model with a constant speciation rate). The ten species of the core clade of *Melinaea* (excluding the most divergent species, *Mel. ludovica*) have diversified in the past 2.84 million years (**Fig. 2B; Fig. S7B**), giving a speciation rate of at least 0.811 speciation events per lineage/My. Of the potential four *Melinaea* species missing in our analysis (*Mel. ethra*, *Mel. mnasias, Mel mnemopsis* and *Mel. scylax*), two likely form part of the core clade, which would increase the speciation rate to 0.875 speciation events per lineage/My.

Both genera thus speciated much faster than the other well-studied Neotropical butterfly radiation of *Heliconius* (0.324 speciation events per lineage/My; 46 species in 11.8 My) (57). Kawahara et al. (35) previously found a significant rate shift towards high diversification rates at the base of ithomiine butterflies (clade L; 0.23 speciation events per lineage/My) and we show that among Ithomiini, *Mechanitis* and *Melinaea* have an even higher speciation rate, consistent with previous results (25).

Signatures of rampant introgression throughout both genera

To examine potential hybridisation between our species, we tested for excess allele sharing between non-sister taxa with Fbranch (**Fig. S8**) and windowed phylogenetic tree discordance with TWISST and IQtree concordance factors. The results of DSuite and TWISST (**Fig. S8; Table S2; Text S2**) are summarised with arrows in **Fig. 2** and the concordance factors indicating how often each clade occurred among the phylogenies as node labels.

There is a signal of rampant hybridisation in *Mechanitis*. The strongest signal is found between *Mec. messenoides* and *Mec. polymnia* (**Fig. 2A - arrow a; Fig. S8A - #1**), which co-occur in Western Amazonia. Hybridisation between these species is also corroborated by the deeply divergent mitochondrial lineages of *Mec. messenoides,* with one of them sister to *Mec. polymnia* (**Fig. 1A - box B**). Another strong signal of excess allele sharing is found between *Mec. menapis* and the clade of *Mec. mazaeus* and *Mec. macrinus* (**Fig. 2A - arrow c; Fig. S8A - #3**). Both *Mec. menapis* and *Mec. macrinus* are found west of the Andes, and the concordance factor support for *Mec. menapis* and its sister species *Mec. messenoides* is only 47.85, indicating potential hybridisation in the West.

There is no excess allele sharing between the *polymnia* lineage west of the Andes and the other *Mec. polymnia* lineages (**Fig. S8A - #5**), indicating that the Andes constitute a strong barrier to gene flow. Nevertheless, we found a single individual in Colombia with equal ancestral contribution of lineages East and West of the Andes (Sal_4944 in **Fig. S1**; **Fig. S9**).

In *Melinaea*, we find hybridisation between various species and low concordance factors at all nodes, even at the base of the core clade (**Fig. 2B**). There is excess allele sharing between *Mel. marsaeus/maeonis* and *Mel. idae, Mel. isocomma, Mel. satevis* and *Mel. mothone* (**Fig. 2B - arrows a-d;**

Fig. S8B - #1-4). It is possible that some of these signals are caused by hybridisation in the ancestor of the *marsaeus/maeonis*-clade, or by an unsampled species closely related to *Mel. marsaeus* and *Mel. maeonis*. In addition, *Mel. idae* has some excess allele sharing with *Mel. lilis* (**Fig. S8B - #5**), which are both found west of the Andes.

Mechanitis nesaea - a putative hybrid species

As the reclassified species *Mec. nesaea* (previously *Mec. lysimnia nesaea*) shows signatures of hybridisation (**Fig. 2A - arrows 4; Fig. S8A - #4A**) and cytonuclear discordance involving its nuclear sister species *Mec. polymnia* and mitochondrial sister *Mec. lysimnia* (**Fig. 1**), we investigated if this species could be of hybrid origin. *Mechanitis nesaea* occurs in the eastern tip of the Brazilian Atlantic Forest. *Mec. lysimnia lysimnia* occurs further south, with a small sympatric zone, and *Mec. polymnia casabranca* largely overlaps with both taxa (**Fig. 2**) (53, 60). An ADMIXTURE analysis shows no recent gene flow between these species (**Fig. S9**), indicating that lysimnia-introgression is likely ancestral to *Mec. nesaea*. However, *Mec. lysiminia lysiminia* and *Mec. polymnia casabranca* have been observed to interbreed in nature (61) and putative hybrids have been found, some resembling *Mec. nesaea* (**Fig. S10**).

Mec. nesaea is intermediate between *Mec. polymnia* and *Mec. lysimnia* in chromosome number (45), lysimnia-like in wing colour patterns and caterpillar phenotypes, although the head capsule colour of later caterpillar instars is sometimes more polymnia-like (58) (**Fig. 3A**). We find that in androconial compounds, *Mec. nesaea* is distinct from both putative parental species but closest to *Mec. polymnia* (**Fig. 3B, Table S3-4**). Some of the differences in androconial compounds might contribute to assortative mating, since some are derivatives of the toxins (PAs) they collect and transfer to females during mating (47, 48). Of the 26 androconial compounds we found, three show very high concentrations, two of which are derivatives of PAs: hydroxydanaidal (peak 2) and methyl hydroxydanaidoate (peak 3) (**Fig. 3C**). The content of these chemicals can vary greatly between individuals, because it depends on the access to PA-containing plants, but we find them to be consistently associated with *Mec. nesaea* and *Mec. p. casabranca* and present only in traces in *Mec. l. lysimnia* (across 92 individuals total from multiple locations, **Table S3**), consistent with previous findings of *Mec. l. lysimnia* (48). On the other hand, heptacosene (peak 12) was dominant in *Mec. l. lysimnia* while only present as traces in *Mec. nesaea* and absent in *Mec. p. casabranca* samples.

To study genomic signatures of differentiation and introgression, we resequenced 15 *Mec. nesaea*, 19 *Mec. l. lysimnia* and 9 *Mec. p. casabranca*, of which many were sampled from sympatry. A multispecies coalescent-with-introgression model indicates that there may already have been some

divergence between *Mec. polymnia* and the polymnia-like ancestor of *Mec. nesaea*, before introgression from *Mec. lysimnia* (**Fig. 3D; Fig. S11**). An F_{ST} analysis in 20kb-windows shows low genome-wide F_{ST} between *Mec. nesaea* and its sister species *Mec. polymnia* from Brazil (0.24) with distinct peaks of high differentiation (**Fig. 3E**). Many of these high-differentiation peaks coincide with genomic regions showing strong introgression between *Mec. lysimnia* and *Mec. nesaea* (**Fig. 3E**), indicating that lysimnia-introgression might have contributed to reproductive isolation between *Mec. nesaea* and *Mec. polymnia*. This is further supported by lysimnia-introgression outliers showing elevated D_{XY} and Population Branch Statistic values (PBS), *i.e.* differentiation of *Mec. nesaea* from both sympatric and allopatric *Mec. polymnia* (**Fig. 3E**, **Fig. S12**). A similar hybrid speciation scenario has recently been proposed for another mimetic butterfly species, *Heliconius elevatus* (62).

Furthermore, some of the F_{ST} peaks coincide with chromosomal breakpoints (**Fig. 3E,** see also 'chromosomal rearrangements'). Future studies should test if high-differentiation peaks with signatures of lysimnia-introgression harbour reproductive isolation barriers such as genes contributing to chemoreception differences.

Chromosomal rearrangements

To study chromosomal rearrangements, we used two published *Melinaea* genomes (63) and generated chromosome-level genomes of three additional *Melinaea* and five *Mechanitis* species using PacBio and HiC-data, resulting in high quality genomes with >96% BUSCO completeness and >94% of the genome assembled in chromosomes (**Table S5-S6**). The *Mechanitis* genomes are substantially shorter (291-320 Mb) than the *Melinaea* genomes (496-661 Mb, **Table S5**).

Whereas most Lepidoptera have highly conserved karyotypes with 31 chromosomes (64, 65), our *Mechanitis* and *Melinaea* genomes are highly rearranged, corroborating earlier findings (63). We performed a synteny analysis using BUSCO genes and the nymphalid *Melitaea cinxia* as representative of the 31 ancestral linkage groups termed Merian elements (**Fig. S13**) (65). The synteny analysis revealed many chromosomal fusions and fissions (**Fig. 4A**), even between closely related sister species. Compared to the Merian elements, the minimum number of fissions (number of chromosomes containing parts of each Merian element) ranged from 74 in *Mec. menapis* to 96 in *Mel. ludovica*, while the number of fusions (Merian elements per chromosome) ranged from 85 *Mec. menapis* to 105 *Mel. ludovica* (**Fig. 4A**). The median length of conserved blocks is 32-36 genes, compared to 168 genes in the outgroup *Danaus plexippus* (**Table S7; Fig. S14**). In most Ithomiini genomes, the canonical Z has not undergone any fissions and shows the longest conserved blocks (229-248 genes, **Fig. 4A, Table S7)**, but has fused with the

ancestral autosome 10 (**Table S8**). We find additional Z-autosome fusions in multiple species (**Table S8**). In many taxa, sex chromosomes play a disproportionate role in speciation (Haldane's rule and/or large-Z effect) and these enlarged sex chromosomes may thus constitute particularly strong barriers to gene flow (66).

To study if chromosomal rearrangements contributed to the rapid diversification of these genera, we mapped the location of the chromosomal breakpoints between all species pairs to test for an association between breakpoints and reduced gene flow. We found increased F_{ST} and reduced diversity (□) in breakpoint regions in all *Mechanitis* comparisons (**Fig. 4B, Fig. S15, Table S9**), including the putative hybrid species *Mec. nesaea* and its sister species *Mech. polymnia* (**Fig. 3E**). This could indicate reduced gene flow at breakpoints. In principle, elevated F_{ST} could also be caused by increased background selection as recombination tends to be reduced at chromosome ends (67, 68). However, we also find elevated absolute divergence (D_{XY}) in windows coinciding with breakpoints in more than half of the comparisons, which indicates that background selection alone cannot explain the pattern (69). In *Melinaea*, we found the same patterns in a majority of the comparisons (**Table S9**).

Reduced or complete absence of recombination at the breakpoints could act as a barrier to gene flow (70) and has also been found in *Brenthis* butterflies (71). At breakpoints meiotic crossover may be impaired due to reduced sequence homology either because of loss of sequence or the presence of telomeric sequences in the split versus fused chromosomes. The resulting reduced recombination could facilitate accumulation of alleles under divergent selection, and rearrangements may thereby facilitate speciation as proposed e.g. for ascomycetous fungi (72).

The complex chromosomal rearrangements in *Melinaea* and *Mechanitis* may constitute barriers to gene flow, particularly at breakpoint regions, in line with findings of nearly sterile hybrids in a cross between two *Melinaea* sister species (46). Also in other butterflies, rearrangements have been suggested to contribute to speciation (13, 67, 73, 74). Nevertheless, some of our genomes showed heterozygosity for fission-fusion rearrangements, indicating within-population variation in karyotype (**Table S5**). This may be akin to *Leptidea sinapis*, where, despite multiple fusion/fission polymorphisms segregating within populations (75, 76), crosses between chromosomal extremes show low survival of F2 hybrids (77). That complex chromosomal rearrangements involving multiple chromosomes likely constitute the strongest barriers to gene flow has also been found, e.g. in shrews (78) and wallabies (79).

Discussion

The natural history of ithomiine butterflies has been studied for over 150 years. They are prime models for Müllerian mimicry (33), and have long been considered biodiversity indicators, as the distribution of threats and refuges for their biodiversity is consistent with trends observed for other biological groups (24, 27, 80, 81). The study of these particularly recent radiations has been hampered by taxonomic challenges. However, our combination of whole-genome resequencing with vast taxonomic and geographic coverage, genome assemblies and detailed androconial chemical analysis of a putative hybrid species, allowed us to resolve taxonomic issues, and also shed light on potential drivers of their diversification. While adaptation to divergent niches and assortative mating likely contribute to species coexistence, our data suggest that geographic isolation, hybridisation-derived genetic variation, and chromosomal rearrangements may have sped up these processes.

The divergence times of *Mechanitis* and *Melinaea* species match a potential effect of Pleistocene climatic fluctuations (2.58 Ma-11.7 ka) in driving diversification. Moreover, we find that many sister species are restricted to different geographic regions, either matching postulated Pleistocene refugia (23, 41, 42) or separated by the Andes. These patterns suggest a potential role of accumulation of differences in allopatry, particularly in small populations like refugial populations. The high rates of chromosomal rearrangements in *Mechanitis* and *Melinaea* likely speed up the accumulation of chromosomal differences in isolated populations. Once coming together in secondary sympatry, low hybrid fitness might then reinforce assortative mating e.g. based on pheromones (32). The putative hybrid species *Mec. nesaea* suggests that hybridisation also contributed to speeding up the diversification. It is possible that *Mec. nesaea* was an isolated population of *Mec. polymnia* that became reproductively isolated from other polymnia-populations due to introgression from *Mec. lysimnia*. Given the high number of introgression events our genomic data revealed across both genera, hybridisation may also have sped up adaptation in general by boosting the genetic variation as seen in other systems (e.g. 5, 7). For instance, in *Heliconius* butterflies it has been shown that introgression contributed to both mimicry ring switches and colour-based assortative mating (82).

Our findings are consistent with the speciation pump hypothesis, postulating that periods of allopatry, followed by secondary sympatry can facilitate diversification (23), as proposed e.g. in fishes (7, 22), or Andean plants (83). Our study highlights that hybridisation in secondary sympatry and increased rates of accumulation of reproductive isolation, e.g. due to high rates of chromosomal rearrangements, can further fuel the speciation pump.

Materials and methods

Collecting butterfly specimens

157 specimens of *Mechanitis*, 9 specimens of *Forbestra*, 105 specimens of *Melinaea,* 1 *Eutresis* and 1 *Olyras* were collected over the years 2000 to 2023 across Central and South America (**Table S1**). Adult butterflies were caught with a net, and their bodies were subsequently preserved in ethanol, DMSO or flash-frozen and stored at -70°C. Moreover, a few legs from dried museum specimens were used (Florida Natural History Museum; Natural History Museum London). Wings were photographed and stored in envelopes. The resulting dataset covers almost all species of *Melinaea* and *Mechanitis* from a wide geographical range. In addition, 65 individuals of *Mec. lysimnia nesaea* (**status restored** to *Mec. nesaea* in this paper; hereafter called *Mec. nesaea*), 19 *Mec. lysimnia lysimnia* and 8 *Mec. polymnia casabranca* were collected for the androconial chemical analysis (**Table S3**).

DNA extractions & whole genome resequencing

DNA extractions were done with either the Qiagen MagAttract High Molecular Weight kit (Qiagen ID 67563), or the Qiagen QiaAmp DNA mini kit (51304), or a PureLink digestion and lysis step followed by a magnetic bead DNA extraction (84). The dried museum specimens were extracted using a Lysis-C buffer and a MinElute DNA extraction kit (protocol adapted from (85); Qiagen ID 28006). Library preparations were performed using homemade TN5-transposase-mediated tagmentation (protocol adapted from (86)), or following the manufacturer's guidelines with the Illumina DNA PCR-free library prep kit and sequenced (150 bp paired-end) on Illumina NovaSeq 6000 or NovaSeq X machines at Novogene or the Wellcome Sanger Institute.

Reference genomes

Reference genomes were assembled for five species of *Mechanitis* and three species of *Melinaea* which were combined with two previously published *Melinaea* genomes (63). In short, we combined 12-57x PacBio HiFi sequencing and 33-197x Illumina sequencing of HiC libraries (haploid coverages, **Table S5**) and assembled the genomes according to the Tree of Life pipelines (https://github.com/sanger-tol/genomeassembly**)** (more details in **Text S3**).

Whole genome mapping

To prepare the whole genome data for analysis, the quality of the reads was checked with FastQC (v0.11.9) (87). Sequences below 50 bp were discarded and adapters and PolyG-tails were trimmed with FastP

(v0.23.2) (88), before they were aligned to a *Melinaea marsaeus* reference (63) or our *Mechanitis messenoides* reference using BWA-mem (v.0.7.17) (89). Picard was used to remove PCR duplicates (v3.0.0) (90). Samtools (v1.17) (91) and GATK3 HaplotypeCaller (v3.8.1.0) (92, 93) were used for variant calling, with a minimum base quality score of 20.

VCFtools (v0.1.16) (94) was used for filtering. Based on the distribution of sequencing depth (mean *Melinaea*: 7; *Mechanitis*: 15), all sites with a mean depth below 3 (*Melinaea*) or 5 (*Mechanitis*), and above 15 (*Melinaea*) or 30 (*Mechanitis*) were removed. Insertions, deletions, sites with >50% missing data, as well as genotypes with a depth below 2 (*Melinaea*) or 3 (*Mechanitis*) were removed. The mitochondrial DNA was filtered separately, with a maximum depth of 1700 (*Melinaea*) or 1200 (*Mechanitis*).

Phylogenetic analyses

For each genus, we ran a Principal Component Analysis (PCA) using Plink (V1.9) to explore population structure (95) (**Fig. S16**). Next, we inferred a phylogenetic tree based on a filtered subset of the whole genome sequence data (thinned to 1 in 500 sites, with a minimum genotype quality of 10). Our filtered VCF-files were converted to phylip with a custom script (vcf2phylip.py, http://www.github.com/joanam/scripts), and subsequently, IQtree2 (v2.1.2) (96) produced phylogenetic trees with ultrafast bootstrap approximation (-B 1000; UFBoost) (97) and the GTR-model.

We inferred separate phylogenies for the mitochondrial and the nuclear DNA. The nuclear trees are based on 537,500 SNPs for *Mechanitis* and 784,526 SNPs for *Melinaea*. The mitochondrial phylogenies are based on the full mitochondrial genome including 11,818 bp for *Mechanitis* and 11,815 bp for *Melinaea.* For *Mechanitis*, we included a maximum of six individuals of the same subspecies and country in the phylogenetic analyses, thus excluding several Brazilian *Mec. polymnia*, *Mec. nesaea* and *Mec. lysimnia*. These individuals were included in hybridisation-analyses. For *Melinaea*, all individuals were used.

In addition, a phylogenetic tree calibrated with divergence times from (25) was produced using the IQtree2 dating options. Divergence between *Forbestra* and *Mechanitis* (5.22 MYA), and *Mechanitis mazaeus* and *Mechanitis macrinus* (0.39 MYA) were used for secondary calibration. For *Melinaea*, we specified the divergence times between *Mel. ludovica* and *Mel. menophilus* (4.66 MY), as well as *Mel. isocomma* and *Mel. lilis* (0.65 MY). The phylogeneties were visualised using the packages 'ape' (v5.7-1) and 'phytools' (v2.1-1) in R (98, 99) and FigTree (v1.1.4) (http://tree.bio.ed.ac.uk/software/figtree/). To calculate a constant speciation rate (λ) we assumed a pure birth model, with n as the number of species and T the time from root to tip: $\square = \square^{\square * \square}$ which gives $\lambda = \square\square(\square)/\square$.

Distribution maps

The coordinates of our individuals and the individuals from (24) were plotted using the libraries 'sf', 'tmap', 'tmaptools' and 'mapview' in R (100–102). We classified the subspecies of (24) into species following our taxonomic revision. Our individuals were plotted as dots on top of the overall distribution combining data with (24). The basemap 'Esri.WorldTerrain' was used, provided through 'Leaflet' (ESRI, ARCGIS; https://github.com/leaflet-extras/leaflet-providers); **Fig. S5-6** has maps including the attribution.

Window trees

IQtree2 was used to produce phylogenetic trees in windows across the genome (one 20kb window every 200kb) and to calculate gene concordance factor between these window-trees and the whole-genome phylogenetic tree (103). TWISST (104) and TWISST'nTERN (105) were used to analyse tree discordance across the genome.

DSuite analysis

We explored excess allele sharing between species or divergent subspecies using DSuite (106). Dtrios calculated D and f4-ratio statistics for all trios and Fbranch then summarised them as f-branch statistics using a species tree based on the nuclear phylogeny of **Fig. 2** (**Table S1**). The results of this analysis were visualised with a python script provided by DSuite.

Genome scans

F_{ST}, D_{XY} and pi were calculated in all species pairs in 20kb windows (including monomorphic sites, with a minimum of 10,000 sites per window) across the genome with the scripts from Simon Martin (https://github.com/simonhmartin/genomics_general).

Admixture and F_{ST} regarding Mec. nesaea

To test for genomic differentiation between the putative hybrid species, *Mec. nesaea* and its closest relative *Mec. polymnia* (nuclear phylogeny), we additionally performed a Population Branch Statistic (PBS) analysis based on F_{ST} between *Mec. polymnia casabranca* (putative parental species in Brazil), *Mec. polymnia chimborazona* (West of the Andes, allopatric), and *Mec. nesaea*. In contrast to F_{ST}, which increases if either of the compared populations experience selection or reduced gene flow, PBS allows to identify genomic regions particularly differentiated in one population compared to two other populations.

By using an allopatric population of *Mec. polymnia*, we can identify genomic regions differentiated due to an allele frequency shift or reduced variation within *Mec. nesaea* specifically. We ran PBScan (107) on non-overlapping windows of 50 SNPs with the filtering options -min 5 (at least 5 individuals per population must have data) and -maf 0.05 (minor allele frequency of at least 0.05) and once specifying -div1 (F_{ST}) and once div2 (D_{XY}).

Next, we used f_{dM} to test if genomic regions of high differentiation in *Mec. nesaea* are potentially due to introgression from *Mec. lysimnia*, as expected if *Mec. nesaea* is a hybrid species with ancestry contributions from *Mec. lysimnia* that contribute to speciation of *Mec. nesaea* from *Mec. polymnia*. We used the script by Simon Martin (ABBABABAwindows.py, https://github.com/simonhmartin/genomics_general) to compute f_{dM} (108) with P1=*Mec. polymnia casabranca* (Brazil), P2=*Mec. nesaea*, P3=*Mec. lysimnia* Brazil, P4=*Mec. messenoides*. We also tested other outgroups (*Forbestra*) and other *Mec. polymnia* and other *Mec. lysimnia* populations, which gave consistent results. High values indicate introgression between *Mec. lysimnia* and *Mec. nesaea*.

Androconial Chemistry

We obtained samples of the androconial secretions from 92 males (**Text S3**). To exclude non-androconial compounds from our analyses, for each population the same extraction procedure was adopted with wings of conspecific females and two non-androconial wing areas of males. Eight solvent negative controls were also taken for each sampling event.

The peak areas of each chromatogram were integrated with MSD ChemStation E.02.01.1177 (Agilent Technologies, USA) to obtain the total ion current signals. A series of linear alkanes (C7–C40) was used to determine the linear retention indices (RI) of each compound (109). Compounds were identified by comparing their mass spectra and retention indices with those of reference samples available from personal and commercial mass spectral libraries (FFNSC 2, MassFinder 4, NIST17, MACE v.5.1 (110), and Wiley Registry™ 9th ed.). The peaks exclusive to the androconial samples were used to determine the relative percentages of each compound per sample.

Dihydropyrrolizines, such as hydroxydanaidal or methyl hydroxydanaidoate, are typically accompanied by smaller peaks formed by degradation during GC/MS analyses and/or storage (48). These degradation peaks were excluded from the generated ion chromatograms and statistical analysis. To avoid non-evident contaminants, we only considered compounds present in more than three individuals for any given taxon.

The data were plotted in R (111) using the vegan package (https://doi.org/10.32614/CRAN.package.vegan) for nonmetric multidimensional scaling with 'monoMDS', specifying a global model, square root transformation and Wisconsin double standardisation (autotransform=TRUE).

Demographic modelling

The hypothesis of a hybrid origin of *Mec. nesaea* was tested using a multispecies-coalescent-with-introgression (MSCi) model implemented in BPP v.4.6.2 (112), with one individual of each of the Brazilian populations (*Mec. nesaea, Mec. lysimnia lysimnia*, *Mec. polymnia casabranca*). Loci were selected randomly from autosomes, and required to be at least 2 kb apart from annotated exons, a maximum size of 2 kb, and be at least 10 kb from the nearest locus. For each locus, individuals with more than 50% missing data and sites containing missing genotypes or overlapping annotated repetitive elements were filtered out. Only loci at least 800 bp long after filters and without missing individuals were considered. Heterozygous sites were assigned IUPAC codes. Demographic parameters were estimated using a fixed species tree with introgression events (**Fig. S16**). An inverse gamma prior (invG) was applied for all population size parameters θ (α=3; β=0.04) and root age parameter τ (α=3; β=0.06). A beta prior was applied to the introgression probability (ϕ) (α=1; β=1). Three replicate MCMC runs of 1,000,000 iterations, after a burn-in period of 50,000 iterations, sampling every 50 iterations were performed for each dataset. Divergence time was calculated based on 4 generations per year, and a mutation rate of 2.90E-09 as in *Heliconius* (62) (T=τ/mutation rate/generations/million years).

Chromosome rearrangements

Synteny and breakpoint analysis was performed using single copy orthologous genes identified with BUSCO version 5.7.1 with the lineage database lepidoptera_odb10 and otherwise default options (113). To compare large scale rearrangements in the *Mechanitis* and *Melinaea* versus the ancestral linkage groups (Merian elements), we used two outgroup genomes, *Melitaea cinxia* (114) and *Danaus plexippus* (115). The output from BUSCO was filtered with a custom script to contain only complete genes located in chromosome-sized scaffolds and excluding W. Only single copy genes were included with the exception of genes on the neo-Z2 of *Mec. macrinus,* where we also included genes classified as duplicated. The sex linking of Z2 appears to be recent and most of the genes had high similarity to the genes on the corresponding W:s and were therefore classified as duplicated by BUSCO. Genes that were actually duplicated (occurring more than once or present on other chromosomes than W) on the Z2 were

removed. We determined syntenic blocks, excluding single gene translocations, by comparing the position of the BUSCO-genes in each genome against the Merian elements (*Melitaea cinxia*), and visualised the syntenic relationship with the R-package gggenomes (116). Minimum number of fusions were determined by the number of different Merian elements located in every query chromosome and fissions were determined as the number of query chromosomes containing parts of each Merian element for each species. The breakpoints between all species within *Mechanitis* and *Melinaea* was determined by the same principle as above using an all against all approach for each genome to compare the BUSCO-gene positions.

To investigate the association between chromosomal rearrangements and species divergence we mapped the location of the breakpoints between each comparison to the reference genomes *Mec. messenoides* and *Mel. marsaeus*. Divergence and diversity was estimated in 20 kb windows along the genome (detailed above), and each window was assigned to Absent or Present based on the presence of a breakpoint. The difference in mean values of F_{ST}, D_{XY} and between windows with and without breakpoints was tested using wilcox.test in R. The analyses above were performed in R v4.4.0 (111).

Funding

This research was funded with the Wellcome Trust award 220540/Z/20/A, a Branco Weiss Fellowship, a Royal Society University Research Fellowship (URF\R1\221041) and a Bateson Research Fellowship by St John's College, Cambridge awarded to JIM. ESMH was supported by NERC DTP C-CLEAR, the Zoology Department of the University of Cambridge, St John's College, Cambridge, and the Wellcome Sanger Institute PhD programme. CEBN had a PhD Scholarship from Coordenação de Aperfeiçoamento de Pessoal de Nível Superior.

Sample collection was further supported by Leverhulme trust (KW and ME), the Phyllis and Eileen Gibbs Fellowship (ME), ANR SPECREP and CLEARWING (ME, MM), HFSP RGP0014/2016 (ME), a Research Fellowship from the Royal Commission for the Great Exhibition of 1851 and a Royal Society Research Grant (SHM) and Deutsche Forschungsgemeinschaft, Schu984/12-2 (SS).

Acknowledgements

We thank Ismael Aldas and Raúl Aldaz for assistance with catching butterflies in Ecuador and Mario Tuanama and Ronald Mori-Pezo for help with rearing and collecting butterflies in Peru, and Augusto Rosa for sampling support in São Paulo, and John R. MacDonald for sampling in Panama. We thank the Peruvian, Ecuadorian and Brazilian authorities as well as the Museo de Historia Natural in Peru and the Museo

Ecuatoriano de Ciencias Naturales in Ecuador for their support. Many thanks to Dr Blanca Huertas and Robyn Crowther from the Natural History Museum in London (NHMUK) for providing butterfly legs of *Mel. isocomma* and *Mel. mothone* and to Dr Petra Korlevic for assistance with extracting DNA from museum specimens.

Data, materials and software availability

All code and tables underlying the figures are found in our GitHub repository: https://github.com/rapidspeciation/mechanitis_melinaea.

Competing interests: The authors declare no competing interests.

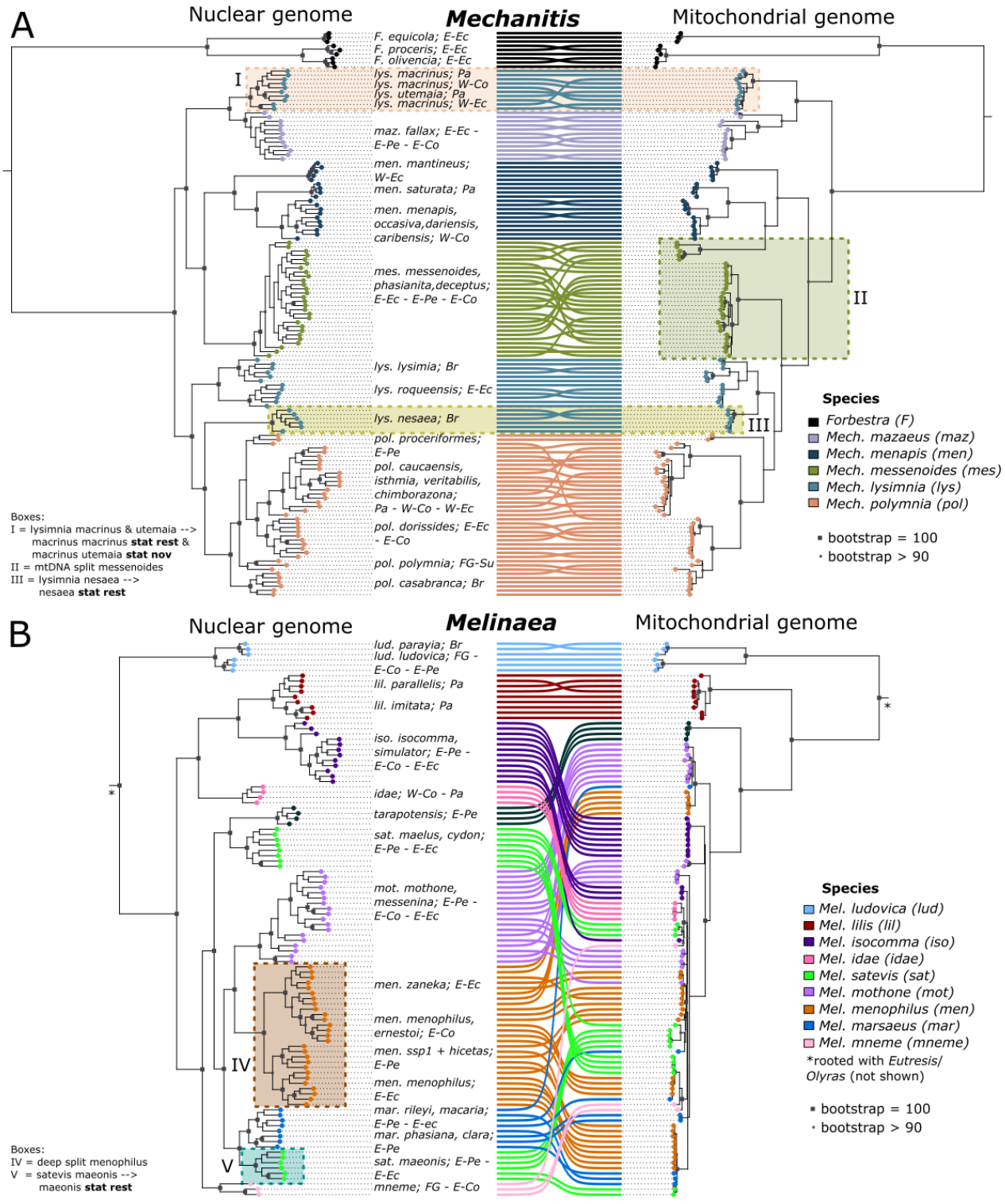

Figure 1 - Rampant cytonuclear discordance in *Mechanitis and Melinaea* and a need for taxonomic revision

Co-phyloplot showing the nuclear and mitochondrial phylogenies of 135 Mechanitis *and 107* Melinaea *individuals. Nuclear phylogeny (left) based on 537,500 SNPs for* Mechanitis *(A) and 784,526 SNPs for* Melinaea *(B) and full mitochondrial genome phylogeny (right). The coloured circles and connecting lines indicate the currently classified species* (37, 54)*. Br=Brazil; FG=French Guiana; E-Co=eastern Colombia; W-Co=western Colombia; E-Ec=eastern Ecuador; W-Ec=western Ecuador; E-Pe=eastern Peru; Pa=Panama, Su=Suriname. The coloured boxes highlight key findings.*

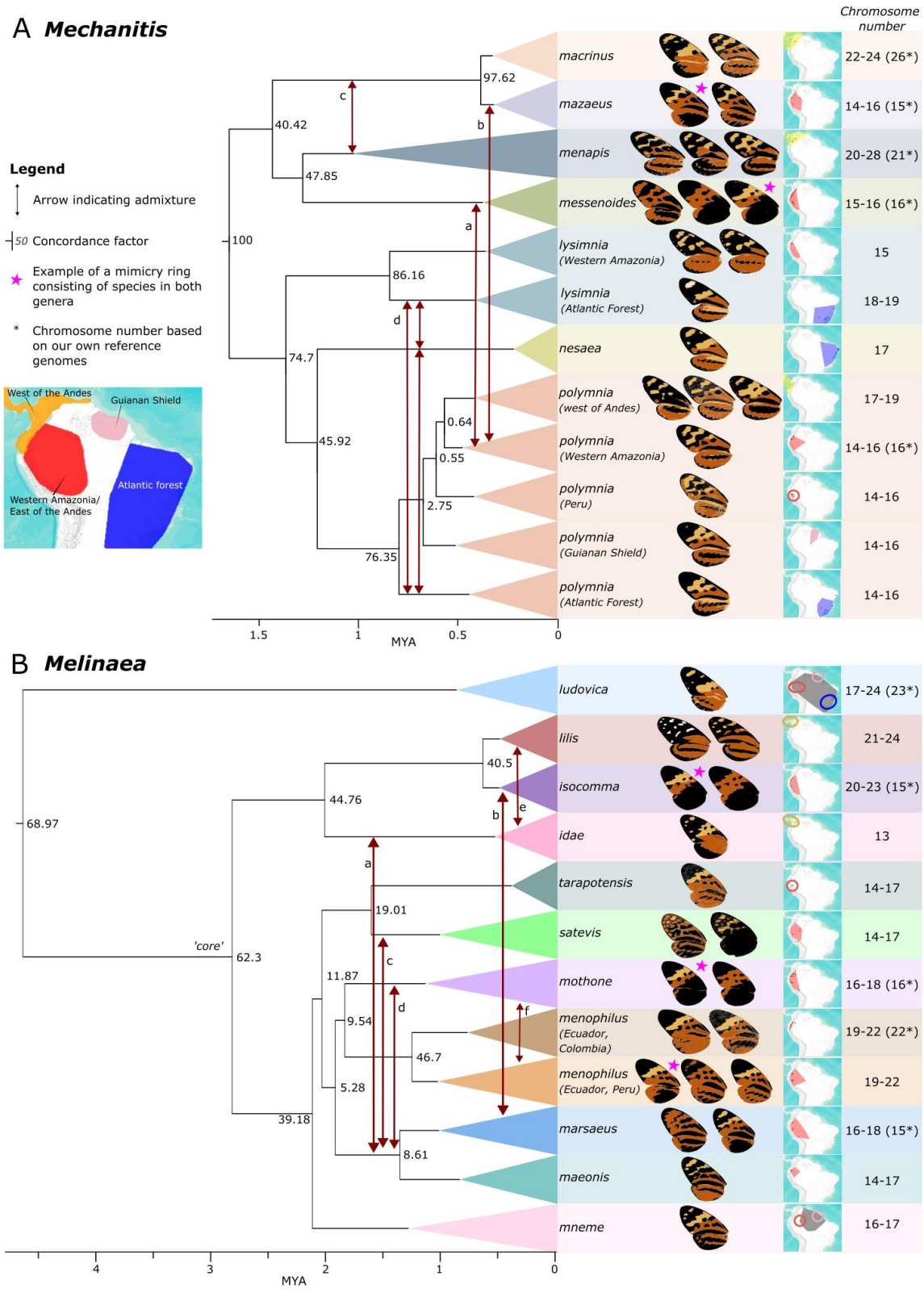

Figure 2 - Calibrated phylogeny of *Mechanitis and Melinaea* butterflies with evidence of introgression and biogeographic patterns.

Time-calibrated phylogenies of Mechanitis *(A) and* Melinaea *(B) with the newly proposed species classification and secondary calibrations from* (25)*. Individuals were collapsed into triangles at the species level or subspecies if they were very divergent. The regions in the overview map are based on the combined distribution of our subspecies and samples from* (24) *with region names adapted from* (25)*. Arrows between clades indicate potential hybridisation events (based on DSuite and TWISST). The node labels indicate IQtree gene concordance factors. 'Core' in the* Melinaea *phylogeny indicates the core clade of fast diverging* Melinaea*. For each clade, cartoon wings based on representative colour patterns are shown, and as an example, pink stars designate taxa part of the same mimicry ring. The distribution of our individuals is indicated by coloured dots and coloured rings on a distribution map based on the subspecies distribution from* (24)*); map from USGS, Esri, TANA, DeLorme and NPS; see* ***Fig. S5-6*** *for larger maps). The chromosome numbers in the right column are based on* (45) *or our reference genomes (asterisk).*

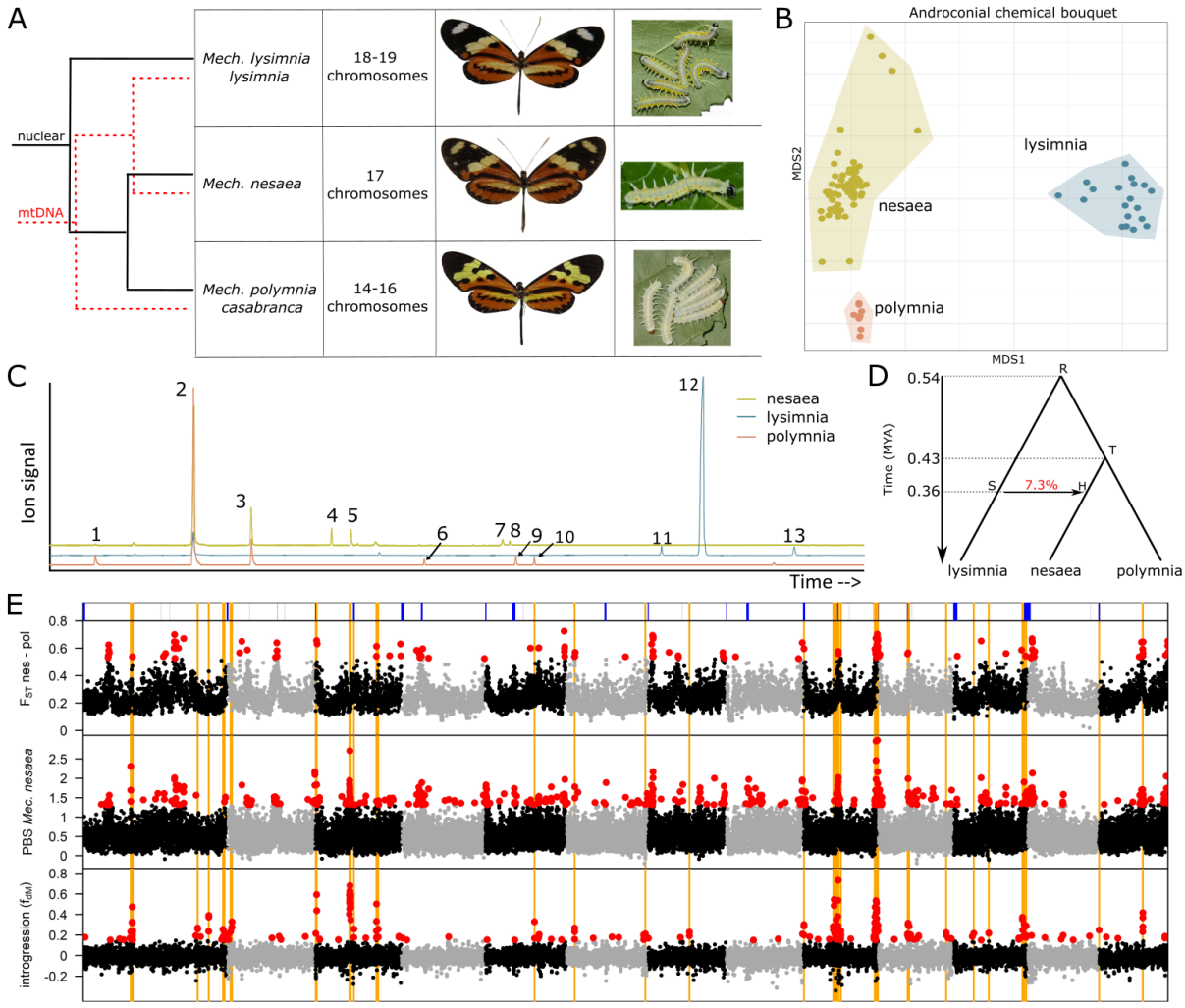

Figure 3 - *Mechanitis nesaea* - a putative hybrid species

The Brazilian Mec. nesaea *is a putative hybrid species between the Brazilian* Mec. lysimnia lysimnia *and* Mec. polymnia casabranca*. Phylogenetic relationships, chromosome numbers* (45)*, a photo of a representative adult and an early fifth instar larva* (58, 59) *are shown in A). The photo of* M. lysimnia lysimia *is a courtesy of Augusto Rosa. B) NMDS shows that the androconial chemical bouquet of* Mec. nesaea *is clearly distinct from both putative parental lineages, most similar to* Mec. polymnia*. **C**) Overlaid chromatograms of androconial extracts of representative individuals of* Mec. nesaea *(yellow line),* Mec. l. lysimnia *(blue) and* Mec. polymnia casabranca *(orange). Peaks: (1) 4-Hydroxy-3,5,5-trimethylcyclohex-2-enone, (2) Hydroxydanaidal, (3) Methyl hydroxydanaidoate, (4) Methyl farnesoate isomer, (5) Methyl (E,E)-farnesoate, (6)* m/z *57, 43, 55, 56, 85, (7) Octadecatrienoic acid (cf.), (8) Octadecanoic acid, (9) Ethyl linolenate, (10)* (E)*-Phytyl acetate (11) Hexacosene, (12) Heptacosene, (13) Nonacosene (not all compounds of **Table S3** are found in these three individuals). **D**) A multispecies coalescent-with-introgression model explored the timing of lysimnia-introgression relative to the divergence times. **E**)*

Genome scans reveal that many genomic regions with high differentiation (F_{ST} and PBS) between Mec. nesaea *and its sister species* Mec. polymnia *show strong signatures of introgression (f_{dM}) between* Mec. nesaea *and* Mec. lysimnia *(P1=polymnia,P2=nesaea,P3=lysimnia,P4=messenoides). Chromosomal breakpoints between* Mec. polymnia *and the four other reference genomes are shown with blue bars on top. Orange vertical lines indicate regions with strong signatures of introgression (top 0.5%). The top 1% windows are highlighted with red large dots in each genome scan.*

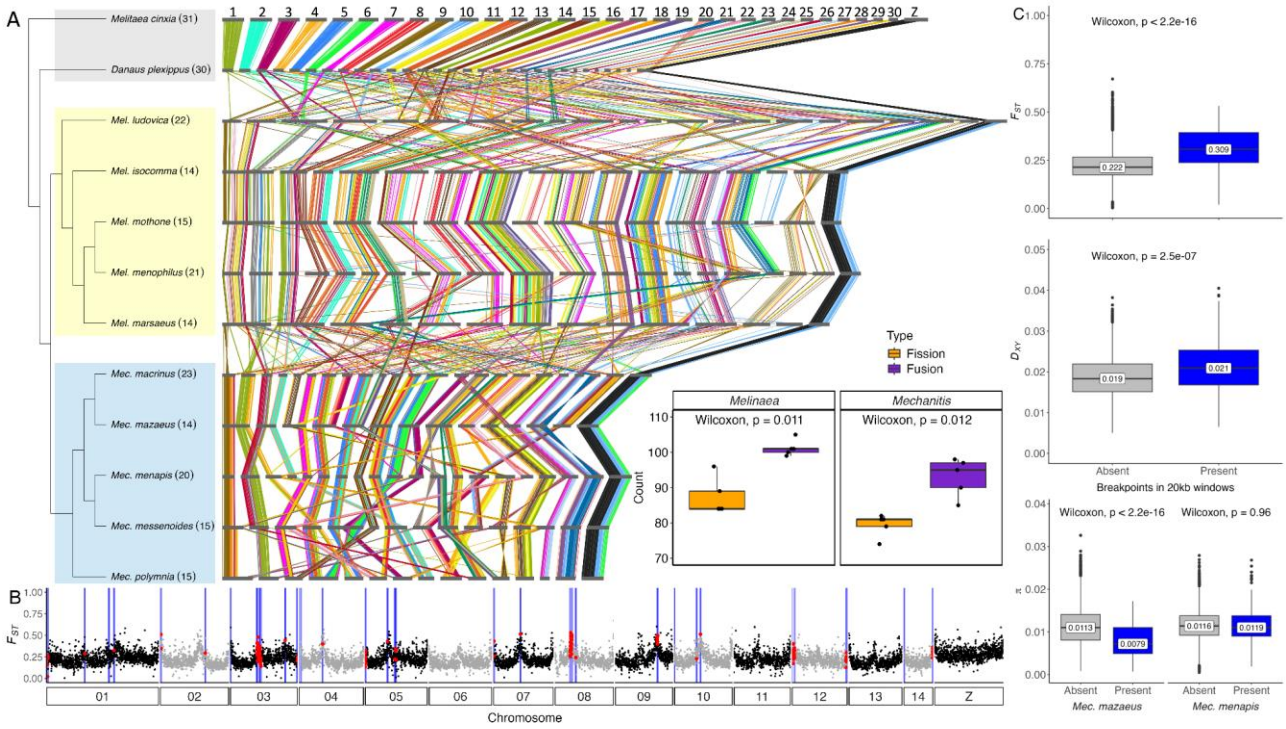

Figure 4 - Chromosomal rearrangements

A) Synteny between Melinaea *(yellow) and* Mechanitis *(blue) genomes based on BUSCO genes positions using* Melitaea cinxia *and* Danaus plexippus *as outgroups (grey). Horizontal bars represent individual chromosomes and vertical links represent BUSCO genes coloured by their ancestral linkage group assignment performed with the reference species* Melitaea cinxia*. The cladogram is based on* ***Fig. 2*** *and shows haploid chromosome numbers (excluding W) in parentheses. Inset: Distribution of minimum number of fissions (orange) and fusions (purple). B) Example of differentiation (F_{ST}) and breakpoints (vertical lines) between* Mec. mazaeus *and* Mec. menapis*. The red dots indicate windows coinciding with breakpoints. C) Boxplots showing the distribution of F_{ST}, D_{XY} and □ in windows with breakpoints present or absent.*

References

1. J. B. Losos, Adaptive radiation, ecological opportunity, and evolutionary determinism : American society of naturalists E. O. Wilson award address. *Am. Nat.* **175**, 623–639 (2010).
2. R. G. Gillespie, *et al.*, Comparing Adaptive Radiations Across Space, Time, and Taxa in *Journal of Heredity*, (Oxford University Press, 2020), pp. 1–20.
3. R. De-Kayne, *et al.*, Why Do Some Lineages Radiate While Others Do Not? Perspectives for Future Research on Adaptive Radiations. *Cold Spring Harb. Perspect. Biol.* a041448 (2024). https://doi.org/10.1101/cshperspect.a041448.
4. R. Abbott, *et al.*, Hybridization and speciation. *J. Evol. Biol.* **26**, 229–246 (2013).
5. D. A. Marques, K. Lucek, V. C. Sousa, L. Excoffier, O. Seehausen, Admixture between old lineages facilitated contemporary ecological speciation in Lake Constance stickleback. *Nat. Commun.* **10** (2019).
6. M. Barrier, B. G. Baldwin, R. H. Robichaux, M. D. Purugganan, Interspecific hybrid ancestry of a plant adaptive radiation: allopolyploidy of the Hawaiian silversword alliance (Asteraceae) inferred from floral homeotic gene duplications. *Mol. Biol. Evol.* **16**, 1105–1113 (1999).
7. J. I. Meier, *et al.*, Cycles of fusion and fission enabled rapid parallel adaptive radiations in African cichlids. *Science* **381**, eade2833 (2023).
8. R. W. R. Wallbank, *et al.*, Evolutionary Novelty in a Butterfly Wing Pattern through Enhancer Shuffling. *PLoS Biol.* **14** (2016).
9. L. H. Rieseberg, *et al.*, Major Ecological Transitions in Wild Sunflowers Facilitated by Hybridization. *Science* **301**, 1211–1216 (2003).
10. J. Mallet, Hybrid speciation. *Nature* **446**, 279–283 (2007).
11. G. L. Bush, S. M. Case, A. C. Wilson, J. L. Patton, Rapid speciation and chromosomal evolution in mammals. *Proc. Natl. Acad. Sci.* **74**, 3942–3946 (1977).
12. A. D. Leaché, B. L. Banbury, C. W. Linkem, A. N.-M. De Oca, Phylogenomics of a rapid radiation: is chromosomal evolution linked to increased diversification in north american spiny lizards (Genus Sceloporus)? *BMC Evol. Biol.* **16**, 63 (2016).
13. J. M. De Vos, H. Augustijnen, L. Bätscher, K. Lucek, Speciation through chromosomal fusion and fission in Lepidoptera. *Philos. Trans. R. Soc. B Biol. Sci.* **375**, 20190539 (2020).
14. K. Lucek, *et al.*, The Impact of Chromosomal Rearrangements in Speciation: From Micro- to Macroevolution. *Cold Spring Harb. Perspect. Biol.* **15**, a041447 (2023).
15. S. Potter, *et al.*, Chromosomal Speciation in the Genomics Era: Disentangling Phylogenetic Evolution of Rock-wallabies. *Front. Genet.* **8** (2017).
16. C. Sotero-Caio, R. Baker, M. Volleth, Chromosomal Evolution in Chiroptera. *Genes* **8**, 272 (2017).
17. J. I. Márquez- Corro, *et al.*, Macroevolutionary insights into sedges (Carex: Cyperaceae): The effects of rapid chromosome number evolution on lineage diversification. *J. Syst. Evol.* **59**, 776–790 (2021).
18. F. J. Ayala, M. Coluzzi, Chromosome speciation: Humans, Drosophila, and mosquitoes. (2005).
19. C. A. Everett, J. B. Searle, B. M. N. Wallace, A study of meiotic pairing, nondisjunction and germ cell death in laboratory mice carrying Robertsonian translocations. *Genet. Res.* **67**, 239–247 (1996).
20. M. A. F. Noor, K. L. Grams, L. A. Bertucci, J. Reiland, Chromosomal inversions and the reproductive isolation of species. *Proc. Natl. Acad. Sci.* **98**, 12084–12088 (2001).
21. L. H. Rieseberg, Chromosomal rearrangements and speciation. (2001).
22. J. April, R. H. Hanner, A.-M. Dion-Côté, L. Bernatchez, Glacial cycles as an allopatric

speciation pump in north-eastern American freshwater fishes. *Mol. Ecol.* **22**, 409–422 (2012).
23. J. Haffer, Speciation in Amazonian Forest Birds: Most species probably originated in forest refuges during dry climatic periods. *Science* **165**, 131–137 (1969).
24. M. Doré, *et al.*, Anthropogenic pressures coincide with Neotropical biodiversity hotspots in a flagship butterfly group. *Divers. Distrib.* **28**, 2912–2930 (2021).
25. N. Chazot, *et al.*, Renewed diversification following Miocene landscape turnover in a Neotropical butterfly radiation. *Glob. Ecol. Biogeogr.* **28**, 1118–1132 (2019).
26. G. W. Beccaloni, K. J. Gaston, Predicting the species richness of neotropical forest butterflies: Ithomiinae (Lepidoptera: Nymphalidae) as indicators. *Biol. Conserv.* **71**, 77–86 (1995).
27. K. S. Brown, “Conservation of Neotropical Environments: Insects as Indicators” in *The Conservation of Insects and Their Habitats*, (Elsevier, 1991), pp. 349–404.
28. K. S. Brown, Adult-obtained pyrrolizidine alkaloids defend ithomiine butterflies against a spider predator. *Nature* **309**, 707–709 (1984).
29. P. J. Devries, F. G. Stiles, Attraction of Pyrrolizidine Alkaloid Seeking Lepidoptera to Epidendrum paniculatum Orchids. **22**, 290–297 (1990).
30. J. R. Trigo, K. S. Brown, Variation of pyrrolizidine alkaloids in Ithomiinae: a comparative study between species feeding on Apocynaceae and Solanaceae. *Chemoecology* **22**, 22–29 (1990).
31. A. V. L. Freitas, *et al.*, Tropane and pyrrolizidine alkaloids in the ithomiinesPlacidula euryanassa andMiraleria cymothoe (Lepidoptera: Nymphalidae). *CHEMOECOLOGY* **7**, 61–67 (1996).
32. M. McClure, *et al.*, Why has transparency evolved in aposematic butterflies? Insights from the largest radiation of aposematic butterflies, the Ithomiini. *Proc. R. Soc. B Biol. Sci.* **286** (2019).
33. F. Müller, Ituna and Thyridia: a remarkable case of Mimicry in Butterflies. *Kosmos* **May**, 100 (1879).
34. J. Mallet, L. E. Gilbert, Why are there so many mimicry rings? Correlations between habitat, behaviour and mimicry in Heliconius butterflies. *Biol. J. Linn. Soc.* **55**, 159–180 (1995).
35. A. Y. Kawahara, *et al.*, A global phylogeny of butterflies reveals their evolutionary history, ancestral hosts and biogeographic origins. *Nat. Ecol. Evol.* **7**, 903–913 (2023).
36. K. R. Willmott, J. Mallet, Correlations between adult mimicry and larval host plants in ithomiine butterflies. *Proc. R. Soc. B Biol. Sci.* **271** (2004).
37. R. I. Hill, *et al.*, Ecologically relevant cryptic species in the highly polymorphic Amazonian butterfly Mechanitis mazaeus s.l. (Lepidoptera: Nymphalidae; Ithomiini). *Biol. J. Linn. Soc.* **106**, 540–560 (2012).
38. N. Chazot, *et al.*, Mutualistic Mimicry and Filtering by Altitude Shape the Structure of Andean Butterfly Communities. *Am. Nat.* **183**, 26–39 (2014).
39. M. McClure, M. Elias, Unravelling the role of host plant expansion in the diversification of a Neotropical butterfly genus. *BMC Evol. Biol.* **16** (2016).
40. I. Birskis-Barros, A. V. L. Freitas, P. R. Guimarães, Habitat generalist species constrain the diversity of mimicry rings in heterogeneous habitats. *Sci. Rep.* **11**, 5072 (2021).
41. K. S. Brown, Quaternary refugia in tropical America: evidence from race formation in *Heliconius* butterflies. *Proc. R. Soc. Lond. B Biol. Sci.* **187**, 369–378 (1974).
42. K. S. Brown, Geographical patterns of evolution in Neotropical Lepidoptera: differentiation of the species of Melinaea and Mechanitis (Nymphalidae, Ithomiinae). *Syst. Entomol.* **2**, 161–197 (1977).
43. K. K. Dasmahapatra, G. Lamas, F. Simpson, J. Mallet, The anatomy of a “suture zone” in Amazonian butterflies: A coalescent-based test for vicariant geographic divergence and

speciation. *Mol. Ecol.* **19**, 4283–4301 (2010).
44. K. K. Dasmahapatra, M. Elias, R. I. Hill, J. I. Hoffman, J. Mallet, Mitochondrial DNA barcoding detects some species that are real, and some that are not. *Mol. Ecol. Resour.* **10**, 264–273 (2010).
45. K. S. Brown, B. V. Schoultz, E. Suomalainen, Chromosome evolution in Neotropical Danainae and Ithomiinae (Lepidoptera). *Hereditas* **141**, 216–236 (2004).
46. M. McClure, B. Dutrillaux, A.-M. Dutrillaux, V. Lukhtanov, M. Elias, Heterozygosity and Chain Multivalents during Meiosis Illustrate Ongoing Evolution as a Result of Multiple Holokinetic Chromosome Fusions in the Genus *Melinaea* (Lepidoptera, Nymphalidae). *Cytogenet. Genome Res.* **153**, 213–222 (2018).
47. J. R. Trigo, K. S. Brown, L. Witte, Pyrrolizidine alkaloids: different acquisition and use patterns in Apocynaceae and Solanaceae feeding ithomiine butterflies (Lepidoptera: Nymphalidae). *Biol. J. Tht Linn. Soc.* **58**, 99–123 (1996).
48. S. Schulz, *et al.*, Semiochemicals derived from pyrrolizidine alkaloids in male ithomiine butterflies (Lepidoptera: Nymphalidae: Ithomiinae). *Biochem. Syst. Ecol.* **32**, 699–713 (2004).
49. P. M. B. Bacquet, *et al.*, Selection on male sex pheromone composition contributes to butterfly reproductive isolation. *Proc. R. Soc. B Biol. Sci.* **282**, 20142734 (2015).
50. M. Elias, *et al.*, Limited performance of DNA barcoding in a diverse community of tropical butterflies. *Proc. R. Soc. B Biol. Sci.* **274**, 2881–2889 (2007).
51. W. T. M. Forbes, A second review of Melinaea and Mechanitis (Lepidoptera, Ithomiinae). *J. N. Y. Entomol. Soc.* **56**, 1–24 (1948).
52. R. M. Fox, A monograph of the Ithomiidae (Lepidoptera). Part II. The Tribe Melinaeini Clark. *Trans. Am. Entomol. Soc.* **86**, 109–171 (1960).
53. R. M. Fox, A monograph of the Ithomiidae (Lepidoptera). Part III. The Tribe Mechanitini. *Mem. Am. Entomol. Soc.* **22** (1967).
54. G. Lamas, Checklist: Part 4A. Hesperioidea - Papilionoidea. *Atlas Neotropical Lepidoptera* **5** (2004).
55. M. McClure, M. Elias, Ecology, life history, and genetic differentiation in Neotropical Melinaea (Nymphalidae: Ithomiini) butterflies from north-eastern Peru. *Zool. J. Linn. Soc.* **179**, 110–124 (2016).
56. A. H. B. Rosa, E. P. Barbosa, N. Wahlberg, A. V. L. Freitas, Systematic position and conservation aspects of Melinaea mnasias thera (Lepidoptera: Nymphalidae: Danainae). *Nat. Conserv. Res.* **9** (2024).
57. K. M. Kozak, *et al.*, Multilocus species trees show the recent adaptive radiation of the mimetic heliconius butterflies. *Syst. Biol.* **64**, 505–524 (2015).
58. M. Carvalho, A. Victor, L. Freitas, E. Barbosa, Immature stages of Mechanitis polymnia casabranca (Nymphalidae, Danainae). (2019). https://doi.org/10.5281/zenodo.2650300.
59. D. H. A. Melo, A. V. L. Freitas, Immature stages of Mechanitis lysimnia nesaea (Nymphalidae: Danainae: Ithomiini). *Trop. Lepidoptera* **33**, 79–85 (2023).
60. L. L. Mota, A. H. B. Rosa, L. R. Vasconcellos, K. R. Willmott, A. V. L. Freitas, A new subspecies of Mechanitis lysimnia from southern Amazonia (Nymphalidae: Danainae: Ithomiini). (2022). https://doi.org/10.5281/zenodo.6604683.
61. J. Vasconcellos-Neto, K. S. Brown, Interspecific Hybridization in Mechanitis Butterflies (Ithomiinae): a Novel Pathway for the Breakdown of Isolating Mechanisms. *Biotropica* **14**, 288 (1982).
62. N. Rosser, *et al.*, Hybrid speciation driven by multilocus introgression of ecological traits. *Nature* **628**, 811–817 (2024).
63. J. Gauthier, *et al.*, First chromosome scale genomes of ithomiine butterflies (Nymphalidae: Ithomiini): Comparative models for mimicry genetic studies. *Mol. Ecol. Resour.* **23**, 872–885 (2023).

64. V. Ahola, *et al.*, The Glanville fritillary genome retains an ancient karyotype and reveals selective chromosomal fusions in Lepidoptera. *Nat. Commun.* **5**, 4737 (2014).
65. C. J. Wright, L. Stevens, A. Mackintosh, M. Lawniczak, M. Blaxter, Comparative genomics reveals the dynamics of chromosome evolution in Lepidoptera. *Nat. Ecol. Evol.* **8**, 777–790 (2024).
66. T. Xiong, *et al.*, A polygenic explanation for Haldane's rule in butterflies. *Proc. Natl. Acad. Sci.* **120**, e2300959120 (2023).
67. S. H. Martin, J. W. Davey, C. Salazar, C. D. Jiggins, Recombination rate variation shapes barriers to introgression across butterfly genomes. *PLOS Biol.* **17**, e2006288 (2019).
68. K. Näsvall, *et al.*, Nascent evolution of recombination rate differences as a consequence of chromosomal rearrangements. *PLOS Genet.* **19**, e1010717 (2023).
69. T. E. Cruickshank, M. W. Hahn, Reanalysis suggests that genomic islands of speciation are due to reduced diversity, not reduced gene flow. *Mol. Ecol.* **23**, 3133–3157 (2014).
70. M. Kirkpatrick, N. Barton, Chromosome Inversions, Local Adaptation and Speciation. *Genetics* **173**, 419–434 (2006).
71. A. Mackintosh, Chromosome Fissions and Fusions Act as Barriers to Gene Flow between Brenthis Fritillary Butterflies. *Mol. Biol. Evol.* **40** (2023).
72. Q. Wang, *et al.*, Extensive chromosomal rearrangements and rapid evolution of novel effector superfamilies contribute to host adaptation and speciation in the basal ascomycetous fungi. *Mol. Plant Pathol.* **21**, 330–348 (2020).
73. F. Cicconardi, *et al.*, Chromosome Fusion Affects Genetic Diversity and Evolutionary Turnover of Functional Loci but Consistently Depends on Chromosome Size. *Mol. Biol. Evol.* **38**, 4449–4462 (2021).
74. H. Augustijnen, *et al.*, A macroevolutionary role for chromosomal fusion and fission in Erebia butterflies. *Sci. Adv.* (2024).
75. V. A. Lukhtanov, V. Dincă, G. Talavera, R. Vila, Unprecedented within-species chromosome number cline in the Wood White butterfly Leptidea sinapis and its significance for karyotype evolution and speciation. *BMC Evol. Biol.* **11**, 109 (2011).
76. L. Höök, K. Näsvall, R. Vila, C. Wiklund, N. Backström, High-density linkage maps and chromosome level genome assemblies unveil direction and frequency of extensive structural rearrangements in wood white butterflies (Leptidea spp.). *Chromosome Res.* **31**, 2 (2023).
77. V. A. Lukhtanov, *et al.*, Versatility of multivalent orientation, inverted meiosis, and rescued fitness in holocentric chromosomal hybrids. *Proc. Natl. Acad. Sci.* **115** (2018).
78. S. Garagna, M. Zuccotti, J. B. Searle, C. A. Redi, P. J. Wilkinson, Spermatogenesis in heterozygotes for Robertsonian chromosomal rearrangements from natural populations of the common shrew, Sorex araneus. *Reproduction* **87**, 431–438 (1989).
79. S. Potter, *et al.*, Limited Introgression between Rock-Wallabies with Extensive Chromosomal Rearrangements. *Mol. Biol. Evol.* **39**, msab333 (2022).
80. A. Paz, *et al.*, Environmental correlates of taxonomic and phylogenetic diversity in the Atlantic Forest. *J. Biogeogr.* **48**, 1377–1391 (2020).
81. K. S. Brown, A. V. L. Freitas, Atlantic Forest Butterflies: Indicators for Landscape Conservation. *Biotropica* **32**, 934–956 (2000).
82. M. Rossi, *et al.*, Adaptive introgression of a visual preference gene. (2024).
83. B. Nevado, N. Contreras- Ortiz, C. Hughes, D. A. Filatov, Pleistocene glacial cycles drive isolation, gene flow and speciation in the high- elevation Andes. *New Phytol.* **219**, 779–793 (2018).
84. M. Kucka, Chan, Yingguang Frank, HMW DNA extraction using magnetic beads. *protocols.io* (2022). https://dx.doi.org/10.17504/protocols.io.b46bqzan.
85. P. Korlević, *et al.*, A Minimally Morphologically Destructive Approach for DNA Retrieval and Whole-Genome Shotgun Sequencing of Pinned Historic Dipteran Vector Species.

Genome Biol. Evol. **13**, evab226 (2021).
86. S. Picelli, *et al.*, Tn5 transposase and tagmentation procedures for massively scaled sequencing projects. *Genome Res.* **24**, 2033–2040 (2014).
87. Andrews, S, FastQC: A quality control tool for high throughput sequence data. (2010).
88. S. Chen, Y. Zhou, Y. Chen, J. Gu, Fastp: An ultra-fast all-in-one FASTQ preprocessor in *Bioinformatics*, (Oxford University Press, 2018), pp. i884–i890.
89. H. Li, R. Durbin, Fast and accurate short read alignment with Burrows-Wheeler transform. *Bioinformatics* **25**, 1754–1760 (2009).
90. Picard, Picard Toolkit. *Broad Inst.* (2019). https://broadinstitute.github.io/picard/.
91. P. Danecek, *et al.*, Twelve years of SAMtools and BCFtools. *GigaScience* **10** (2021).
92. A. McKenna, *et al.*, The genome analysis toolkit: A MapReduce framework for analyzing next-generation DNA sequencing data. *Genome Res.* **20**, 1297–1303 (2010).
93. V. Ruano-Rubio, *et al.*, Scaling accurate genetic variant discovery to tens of thousands of samples. (2017). https://doi.org/10.1101/201178.
94. P. Danecek, *et al.*, The variant call format and VCFtools. *Bioinformatics* **27**, 2156–2158 (2011).
95. S. Purcell, *et al.*, PLINK: A tool set for whole-genome association and population-based linkage analyses. *Am. J. Hum. Genet.* **81**, 559–575 (2007).
96. B. Q. Minh, *et al.*, IQ-TREE 2: New Models and Efficient Methods for Phylogenetic Inference in the Genomic Era. *Mol. Biol. Evol.* **37**, 1530–1534 (2020).
97. D. T. Hoang, *et al.*, UFBoot2: Improving the Ultrafast Bootstrap Approximation. *Mol Biol Evol* **35**, 518–522 (2017).
98. L. J. Revell, phytools 2.0: an updated R ecosystem for phylogenetic comparative methods (and other things). *PeerJ* **12**, e16505 (2024).
99. E. Paradis, K. Schliep, ape 5.0: an environment for modern phylogenetics and evolutionary analyses in R. *Bioinformatics* **35**, 526–528 (2019).
100. E. Pebesma, Simple Features for R: Standardized Support for Spatial Vector Data. *R J.* **10**, 439 (2018).
101. M. Tennekes, tmap: Thematic Maps in R. *J. Stat. Softw.* **84** (2018).
102. T. Appelhans, F. Detsch, C. Reudenbach, S. Woellauer, Mapview: Interactive viewing of spatial data in R. *R Package* **version 2.11.2** (2023).
103. B. Q. Minh, M. W. Hahn, R. Lanfear, New methods to calculate concordance factors for phylogenomic datasets. *Mol. Biol. Evol.* **37**, 2727–2733 (2020).
104. S. H. Martin, S. M. Van Belleghem, Exploring Evolutionary Relationships Across the Genome Using Topology Weighting. *Genetics* **206**, 429–438 (2017).
105. S. Stankowski, *et al.*, Selection on many loci drove the origin and spread of a key innovation. [Preprint] (2023). Available at: http://biorxiv.org/lookup/doi/10.1101/2023.02.13.528213 [Accessed 15 June 2024].
106. M. Malinsky, M. Matschiner, H. Svardal, Dsuite - Fast D-statistics and related admixture evidence from VCF files. *Mol. Ecol. Resour.* **21**, 584–595 (2021).
107. T. Hämälä, O. Savolainen, Genomic Patterns of Local Adaptation under Gene Flow in Arabidopsis lyrata. *Mol. Biol. Evol.* **36**, 2557–2571 (2019).
108. S. H. Martin, J. W. Davey, C. D. Jiggins, Evaluating the Use of ABBA–BABA Statistics to Locate Introgressed Loci. *Mol. Biol. Evol.* **32**, 244–257 (2015).
109. H. van D. Dool, P. D. Kratz, A generalization of the retention index system including linear temperature programmed gas-liquid partition chromatography. *J. Chromatogr. A* **11**, 463–471 (1963).
110. S. Schulz, A. Möllerke, MACE – An Open Access Data Repository of Mass Spectra for Chemical Ecology. *J. Chem. Ecol.* **48**, 589–597 (2022).
111. R Core Team, A language and environment for statistical computing. *R Found. Stat. Comput.* (2024). https://doi.org/10.1080/01621459.1972.10481279.

112. T. Flouri, X. Jiao, B. Rannala, Z. Yang, A Bayesian Implementation of the Multispecies Coalescent Model with Introgression for Phylogenomic Analysis. *Mol. Biol. Evol.* **37**, 1211–1223 (2020).
113. M. Manni, M. R. Berkeley, M. Seppey, F. A. Simão, E. M. Zdobnov, BUSCO Update: Novel and Streamlined Workflows along with Broader and Deeper Phylogenetic Coverage for Scoring of Eukaryotic, Prokaryotic, and Viral Genomes. *Mol. Biol. Evol.* **38**, 4647–4654 (2021).
114. R. Vila, *et al.*, The genome sequence of the Glanville fritillary, Melitaea cinxia (Linnaeus, 1758). *Wellcome Open Res.* **6**, 266 (2021).
115. L. Gu, *et al.*, Dichotomy of Dosage Compensation along the Neo Z Chromosome of the Monarch Butterfly. *Curr. Biol.* **29**, 4071-4077.e3 (2019).
116. T. Hackl, M. J. Ankenbrand, B. van Adrichem, gggenomes: a grammar of graphics for comparative genomics. *R Package* (2024). https://github.com/thackl/gggenomes.